# Second order nonlinear optical properties of In-doped lithium niobate

D. Xue, K. Betzler,[a] and H. Hesse

*Fachbereich Physik, Universität Osnabrück, D-49069 Osnabrück, Germany*

Second order nonlinear optical properties of In-doped lithium niobate crystals have been quantitatively studied from the chemical bond viewpoint. The results show that the second order nonlinear optical response of In-doped lithium niobate crystals at 1079 nm decreases remarkably with increasing In concentration in the crystal. This approximately linear composition-property correlation in In-doped lithium niobate crystals is quantitatively expressed in the current work. Furthermore, the different influences of Mg, Zn, and In dopants, respectively, on the nonlinear susceptibility of lithium niobate single crystals are also compared in the present work. © *2001 American Institute of Physics.* [DOI: 10.1063/1.1336562]

## I. INTRODUCTION

Due to its large electro-optical and nonlinear optical coefficients,[1,2] lithium niobate, $LiNbO_3$, is an important crystal material widely used for numerous optical applications (e.g., for holographic memories, photorefractive devices, waveguide structures, electro-optic modulators, frequency doublers and mixers, parametric oscillators, etc.). Various trivalent ions, such as transition metals and rare earth elements, belong to the most important impurities in lithium niobate because of their essential influence on the properties of this material (photorefractive properties, electro-optic coefficients, light absorption, refractive indices, etc.) and thus their consequences for present and future applications. In various doped lithium niobate single crystals, people have successfully proven that although nominally pure lithium niobate devices are damaged under high intensity illumination due to the photorefractive effect, the problem can be greatly reduced by codoping lithium niobate single crystals with $MgO$,[3] $ZnO$,[4] or $In_2O_3$,[5] etc. Obviously, knowledge of the lattice environment and the chemical state of such dopants is essential for a quantitative understanding of the impurity effects from both theoretical and experimental aspects. Therefore, investigations on extrinsic (i.e., impurities) and intrinsic defects (e.g., Li vacancies) in lithium niobate have been of great interest and led to some interesting conclusions.[6–10] Lithium niobate is usually grown with congruent, nonstoichiometric composition, exhibiting a certain Li deficit. Newer measurements confirm that the Li vacancy model seems reasonable in describing the intrinsic defect structure of nonstoichiometric lithium niobate single crystals,[11] and that most dopants (except Ta and W) prefer to occupy Li sites in oxygen octahedra along the trigonal symmetry axis of the crystal.[7,12] Recently reported results show that in In-doped lithium niobate crystals the In dopants are more or less in similar physicochemical states as Li ions in pure lithium niobate crystals.[13] Therefore, we can do some theoretical predictions of physical properties for In-doped lithium niobate single crystals on the basis of this known

structural behavior. Our previous work has shown how the crystal composition influences its dielectric responses (the refractive indices, and second order nonlinear optical tensor coefficients).[14]

Doping lithium niobate single crystals with $In_2O_3$ (exclusively or combined with additional dopants) leads to a large reduction of the optical damage, due to the influence of $In^{3+}$ on the photorefractive properties of lithium niobate crystals.[5,8,15] At the same time, we also find that other optical properties such as refractive indices[16] and phase-matching conditions for various configurations of second-harmonic generation (SHG)[17] are influenced by In. Until now, the composition influence of In doping on the second order nonlinear optical behavior of lithium niobate single crystals has not been quantitatively investigated. Our previous studies on the Mg-doped[18] and Zn-doped[19] lithium niobate single crystals have quantitatively shown that Mg and Zn dopants have quite obvious influences on the dielectric response of doped lithium niobate crystals. A decrease of all nonvanishing tensor elements of the nonlinear optical susceptibility was found. As for the In dopant atomic size, possible valence and electronic shell configuration are quite different from those of Mg and Zn dopants (both have similar basic characteristics), it is important to analyze the quantitative influence of the In dopant on dielectric responses of In-doped lithium niobate crystals.

Our modified chemical bond method allows us to understand dielectric responses of crystal materials from their corresponding crystallographic structures using the constructed structure−property relationship for crystal materials.[20] In an earlier work,[21] we have quantitatively studied linear and second order nonlinear optical responses of lithium niobate crystals at 1064 nm from their detailed crystallographic structures at room temperature.[22] Based on this, in the present work, the second order nonlinear optical behavior of In-doped lithium niobate at 1079 nm will be quantitatively studied on the basis of the chemical bond viewpoint[20,23] and the constitution−property relationship in crystal materials.[14]

[a]Electronic mail: klaus.betzler@uni-osnabrueck.de

849

## II. THEORETICAL METHOD

As shown in previous works (for an overview see Ref. 20), the chemical bond method regards certain macroscopic physical properties of a crystal as the combination of the contributions of all constituent chemical bonds. A multibond crystal $A_a B_b \ldots$ is split up into constituent bonds $A-B$ with appropriately chosen partial charges. The distribution of the valence electrons over the contributing bonds is defined by the so-called *bond-valence equation* which is derived from the bond graph of the compound (see Sec. III).

To get the (isotropic) *linear* susceptibility of a crystal material, the contributions of all individual scalar linear bond susceptibilities have to be summed up. To get the *nonlinear* susceptibility, the individual tensorial nonlinear bond susceptibilities must be summed up geometrically.

The macroscopic linear susceptibility of a crystal is given by the sum over all contributions and can be written as

$$\chi = \sum_\mu F^\mu \chi^\mu = \sum_\mu N_b^\mu \chi_b^\mu, \tag{1}$$

with $F^\mu$: fraction of bonds of type $\mu$ composing the crystal, $\chi^\mu$: linear susceptibility contribution from $\mu$ type bonds, $N_b^\mu$: number of bonds of type $\mu$ per cm$^3$, $\chi_b^\mu$: susceptibility of a single bond of type $\mu$.

According to Phillips[24] and Van Vechten[25] the linear susceptibility $\chi^\mu$ contributed by the bonds of type $\mu$ in a crystal can be defined as

$$\chi^\mu = (4\pi)^{-1} (\hbar \Omega_p^\mu / E_g^\mu)^2, \tag{2}$$

where $\Omega_p^\mu$ is the plasma frequency and $E_g^\mu$ is the average energy gap between the bonding and antibonding states of the bond. $E_g^\mu$ can be separated into homopolar and heteropolar (i.e., covalent and ionic) contributions $E_h^\mu$ and $C^\mu$

$$(E_g^\mu)^2 = (E_h^\mu)^2 + (C^\mu)^2, \tag{3}$$

$$E_h^\mu = K_1 / (d^\mu)^{2.48}, \tag{4}$$

$$C^\mu = K_2 b^\mu \exp(-k_s^\mu r_0^\mu)[(Z_A^\mu)^* - n(Z_B^\mu)^*] r_0^\mu, \tag{5}$$

where $K_1$ and $K_2$ are constants consisting only of physical fundamental constants like $\hbar, e, \ldots$ and adapted to the units of measure used in the concrete calculation (for lengths in Å and energies in eV, the numerical values are[26] $K_1 = 39.74$ and $K_2 = 14.4$). $d^\mu = 2r_0^\mu$ is the bond length of the bond $A-B$, $\exp(-k_s^\mu r_0^\mu)$ is the Thomas–Fermi screening factor. $(Z_A^\mu)^*$ and $(Z_B^\mu)^*$ are the effective numbers of valence electrons of the two atoms in the bond, $n$ is the ratio of numbers of the two elements $B$ and $A$ in the bond valence equation.[21] Because the true screening behavior in a solid is more complex than this simple Thomas-Fermi description, a correction factor $b^\mu$ is introduced.[25] This factor is also used to correct for $d$-electron influences not accounted for in the effective $Z^*$. These $d$-electron effects on the bond susceptibilities were at first considered by Levine[26] but are still in controversial discussion.[27,28] According to Levine,[29] the different factors $b^\mu$ can be written as $b^\mu = \beta(\bar{N}_c^\mu)^2$ with one global parameter $\beta$ – global for all different bonds in the compound, where $\bar{N}_c^\mu$ is the average coordination number of the ions $A$ and $B$ in the bond $\mu$. If the linear susceptibility, i.e., the refractive index, of a crystal is known, this parameter $\beta$ can be adjusted to describe the linear susceptibility exactly. Thus in general also the results for the nonlinear susceptibility are improved.

The description of the second order nonlinear susceptibility can be derived in a similar way, this was basically done by Levine,[30] extensions for complex crystals were developed by Xue and Zhang.[20] The final result for the second order nonlinear optical tensor coefficients $d_{ij}$ can be written as the appropriate geometric sum over the contributions of all constituent bonds:

$$d_{ij} = \sum_\mu \left\{ \frac{G_{ij}^\mu N_b^\mu (0.5)\{[(Z_A^\mu)^* + n(Z_B^\mu)^*]/[(Z_A^\mu)^* - n(Z_B^\mu)^*]\} f_i^\mu (\chi_b^\mu)^2}{d^\mu q^\mu} + \frac{G_{ij}^\mu N_b^\mu s(2s-1)[r_0^\mu/(r_0^\mu - r_c^\mu)]^2 f_c^\mu (\chi_b^\mu)^2 \rho^\mu}{d^\mu q^\mu} \right\}. \tag{6}$$

The first part denotes the ionic fraction, the second part the covalent fraction of the nonlinear optical coefficient. The meaning of the constants on the right-hand side of Eq. (6) includes:

$G_{ij}^\mu$: geometrical contribution of chemical bonds of type $\mu$,

$N_b^\mu$: number of bonds of type $\mu$ per cm$^3$,

$\chi_b^\mu$: susceptibility of a single bond of type $\mu$,

$(Z_A^\mu)^*$, $(Z_B^\mu)^*$: effective number of valence electrons of $A$ and $B$ ions, respectively,

$n$: ratio of numbers of two elements $B$ and $A$ in the bond valence equation,[21]

$f_i^\mu$, $f_c^\mu$: fractions of ionic and covalent characteristics of the individual bonds, $f_i^\mu = (C^\mu)^2 / [(E_h^\mu)^2 + (C^\mu)^2]$

and $f_c^\mu = 1 - f_i^\mu$, where $C^\mu$, $E_h^\mu$ are the average energy gaps due to ionic and covalent effects,

$d^\mu$: bond length of the $\mu$ type bonds in Å,

$q^\mu$: bond charge of the $\mu$th bond,

$s$: exponent in the bond force constant (2.48),

$r_c^\mu = 0.35 r_0^\mu$: core radius, where $r_0^\mu = d^\mu/2$,

$\rho = (r_A^\mu - r_B^\mu)/(r_A^\mu + r_B^\mu)$: difference in the atomic sizes, where $r_A^\mu$ and $r_B^\mu$ are the covalent radii of atoms $A$ and $B$.

All of the above constants have to be deduced from a structural analysis based on the crystallographic structure and taking into account the detailed chemical bonding situation of
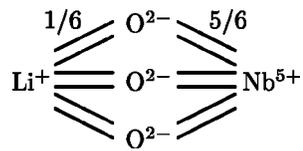
FIG. 1. The bond graph of LiNbO₃. The valences of atoms and theoretical valences of the bonds are shown. Double lines denote two nonequivalent bonds.

all constituent atoms.[20] It should be emphasized that besides the parameter $\beta$ introduced for the linear susceptibility no further adjustable parameters are included.

## III. RESULTS AND DISCUSSION

In order to determine the linear and second order non-linear optical properties of each kind of constituent chemical bond quantitatively, one has to know the detailed bonding environments of all constituent atoms, which are related to the structural characteristics of the assigned crystal. The chemical bond method,[20,23] applied here, treats a compound as an infinite network of constituent atoms linked by chemical bonds. For crystals, due to their periodicity, this can be reduced to a finite network consisting of a single formula unit such as the network of LiNbO₃, the graph of which is shown in Fig. 1. Each line in the graph represents a different bond, $Li^+$ and $Nb^{5+}$ are six-coordinated each and all $O^{2-}$ are four coordinated.

According to the bond-valence model, the charge-neutrality principle in any crystal formula should be obeyed, and each atom shares its valence as equally as possible among the bonds that it forms.[23] Therefore, the following two network equations must always be obeyed:

$$\sum_B s_{AB} = V_A, \quad \text{and} \quad \sum_{\text{loop}} s_{AB} = 0, \tag{7}$$

where each atom $A$ in the corresponding lattice is assigned a formal charge equal to its atomic valence or oxidation state ($V_A$) and each bond between atoms $A$ and $B$ is assigned a bond valence ($s_{AB}$). The sum of the bond valences (each with appropriate algebraic sign according to the bond direction) at each node atom in the network equals its formal charge, the sum around any loop is zero.

In the crystallographic structure of pure lithium niobate single crystals, the ideal cation stacking sequence along the $c$ axis is $\dots -Li-Nb-\square-Li-Nb-\square- \dots$, where $\square$ represents a structural vacancy (an empty octahedron).[22] This ideal stacking sequence (constituent octahedra in pure lithium niobate) is sketched in Fig. 2. However, when $In^{3+}$ cations are introduced as dopants into such a stacking sequence, the situation changes into a different case. Like Mg in Mg-doped LiNbO₃[18] or Zn in Zn-doped LiNbO₃,[19] In dopants also prefer to occupy Li sites, not Nb sites. This could be confirmed recently by the experimental observation of In sites in the crystallographic frame of lithium niobate.[13]

As In adopts a +3 valence state when entering the crystallographic frame, it replaces three Li ions by occupying one of these Li sites and generating two Li vacancies in the near neighborhood. As a result of this replacement, a certain
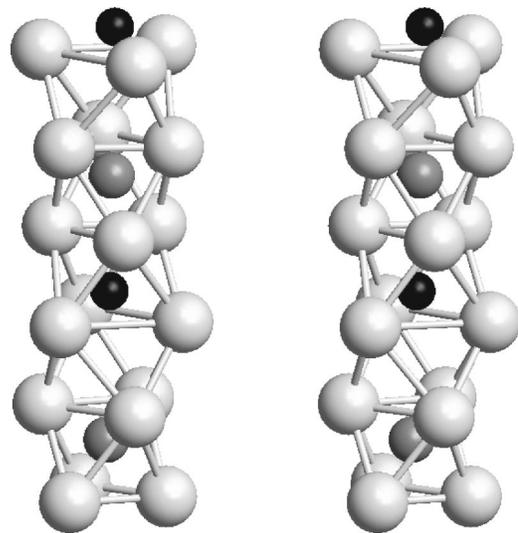


FIG. 2. Stereoscopic view (to be viewed with crossed eyes) of the ideal crystal stacking sequence of lithium niobate along the crystallographic $c$ axis (light gray: oxygen, dark gray: niobium, black: lithium).

lattice relaxation should occur. Yet to date neither experimental nor theoretical data are available describing this relaxation in a reasonable way. Therefore, as a first order approximation suitable for low doping levels, we assume that the lattice parameters around $In^{3+}$ ions are unchanged compared to the ideal lithium niobate lattice. This means that for calculations we can use the identical bond lengths and directions as in the ideal lattice. To reflect the relaxation, refractive index data for In-doped lithium niobate[16] are used as references in calculating the constituent chemical bond parameters.

To facilitate calculations further, we treat In-doped lithium niobate, written as $Li_{1-x}In_{x/3}NbO_3$, formally as a random mixture of $(1-x)$ parts LiNbO₃ and $(x/3)$ parts In Nb₃O₉. Accordingly, calculations for the two components can be treated separately. The results then can be combined linearly using the linear correlation between dielectric responses and constituent atoms in crystal materials shown previously.[14] As a consequence of the two Li vacancies in In Nb₃O₉ when formally applying the same crystal structure like in pure lithium niobate, the bond graph for this material is more complicated than that for lithium niobate. It is sketched in Fig. 3. As in lithium niobate, $In^{3+}$ and $Nb^{5+}$ cations are six-coordinated each, but two types of $O^{2-}$ ions exist, six of them three- and three two-coordinated. Furthermore, according to the two types of $O^{2-}$ ions, Nb–O bonds have to be introduced, which, in addition to different lengths and directions, exhibit different formal charges.

According to the above analysis we calculated the chemical bond parameters [i.e., the constants in Eqs. (1) and (6)] for all types of bonds present in pure lithium niobate and in the above defined ''indium niobate.'' The bond lengths $d^\mu$ are taken from the detailed crystallographic data of lithium niobate.[31] The global fit parameter $\beta$—implicitly contained in all $\chi^\mu$ and $d^\mu_{ij}$—is derived for lithium niobate from the refractive index of pure lithium niobate, for ''indium niobate'' from the refractive indices of In-doped lithium
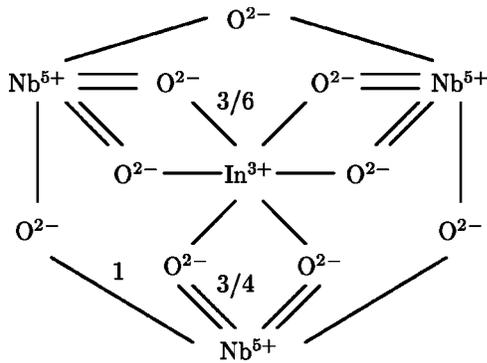
FIG. 3. Bond graph of $InNb_3O_9$. Valences of atoms and theoretical valences of the bonds are shown. The assumption that In replaces three Li ions leads to the ''average'' coordination scheme sketched here. For the calculation of the total susceptibility, an appropriate random sum of the individual bond susceptibilities must be taken.
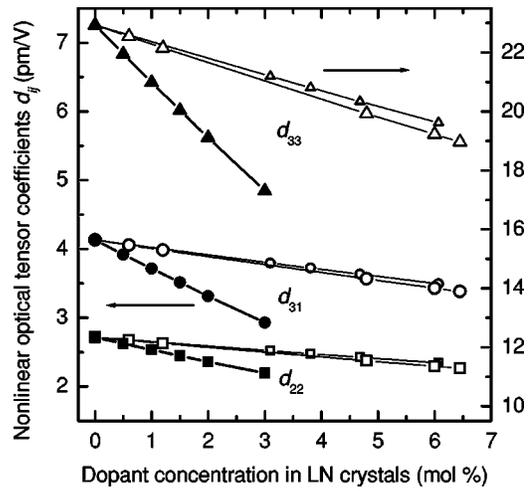


FIG. 4. Nonlinear optical tensor coefficients $d_{ij}$ in doped lithium niobate as a function of the dopant concentration. Filled markers: In doped, small open markers: Zn doped, large open markers: Mg doped lithium niobate.

niobate.[16] No additional fit parameters for the nonlinear susceptibility tensor coefficients are used. The results for all constituent bonds are summarized in Table I (left-hand side: pure lithium niobate, right-hand side: pure ''indium niobate'').

Adding up the individual tensorial contributions of all constituent chemical bonds, we can quantitatively calculate all independent second order nonlinear optical tensor coefficients $d_{22}$, $d_{31}$, and $d_{33}$ at 1079 nm of pure and In-doped lithium niobate as a function of the doping concentration. Our calculated results for pure lithium niobate are $d_{22} = 2.713$ pm/V, $d_{31} = -4.130$ pm/V, and $d_{33} = -22.934$ pm/V, values which agree well with the reported experimental data at 1064 nm as given by Roberts[32] (adopted from Miller *et al.*[33])—$d_{22} = 2.1$ pm/V, $d_{31} = -4.3$ pm/V, $d_{33} = -27$ pm/V—and by Shoji *et al.*[34]—$d_{31} = -4.6$ pm/V, $d_{33} = -25.2$ pm/V—as well as with our previously calculated results at 1064 nm.[21]

Results for In-doped lithium niobate are achieved by replacing a certain amount of lithium niobate with ''indium niobate'' in an appropriate random distribution. The dependencies of the three tensor coefficients on the doping concentration are plotted in Fig. 4, for comparison, the results for Zn- and Mg-doped lithium niobate are included in the plot. All coefficients decrease approximately linearly with increasing doping concentrations. This indicates that the dopants directly or indirectly reduce the acentricity of the material. The decrease is most expressed in In-doped lithium niobate, considerably less in the case of Zn or Mg doping, the ratio of the slopes is approximately 4. One explanation for the large difference between three- and two-valent dopants is the scaling used. The $d$ values are plotted as a function of the ''molar'' impurity concentration which usually is referred to the basic oxides composing the material. These basic oxides are $Li_2O$, $Nb_2O_5$, $MgO$, $ZnO$, and $In_2O_3$, respectively. Taking this and the respective valence state into account, $In_2O_3$ introduces four times as much Li vacancies as $MgO$ or $ZnO$

TABLE I. Calculated chemical bond parameters, linear, and second order nonlinear optical properties of all constituent chemical bonds in In-doped $LiNbO_3$ single crystals $Li_{1-x}In_{x/3}NbO_3$ at 1079 nm. The notation for the bond type includes: (s)–short, (l)–long, (II)–two-coordinated O, (III)–three-coordinated O.

| Bond Type | Constituent chemical bonds in $(LiNbO_3)(1-x)$ | | | | Constituent chemical bonds in $(InNb_3O_9)(x/3)$ | | | | | |
|---|---|---|---|---|---|---|---|---|---|---|
| | Li–O (l) | Li–O (s) | Nb–O (l) | Nb–O (s) | In–O (l) | In–O (s) | Nb–O (II l) | Nb–O (III l) | Nb–O (II s) | Nb–O (III s) |
| $d^\mu$ (Å) | 2.245 | 2.063 | 2.130 | 1.876 | 2.245 | 2.063 | 2.130 | 2.130 | 1.876 | 1.876 |
| $f_c^\mu$ | 0.649 | 0.666 | 0.220 | 0.226 | 0.277 | 0.287 | 0.356 | 0.196 | 0.368 | 0.207 |
| $\chi^\mu$ | 3.132 | 2.705 | 5.603 | 4.475 | 3.032 | 2.655 | 7.723 | 2.906 | 6.200 | 2.378 |
| $q^\mu/e$ | 0.180 | 0.199 | 0.536 | 0.641 | 0.505 | 0.557 | 0.482 | 0.778 | 0.580 | 0.898 |
| $G_{22}^\mu$ | −0.027 | −0.014 | −0.032 | 0.065 | −0.027 | −0.014 | −0.032 | −0.032 | 0.065 | 0.065 |
| $d_{22}^\mu \left(\dfrac{pm}{V}\right)$ | 2.029 | 0.775 | 0.201 | −0.292 | 0.121 | 0.051 | 1.575 | 0.017 | −2.067 | −0.046 |
| $G_{31}^\mu$ | 0.176 | −0.152 | −0.184 | 0.183 | 0.176 | −0.152 | −0.184 | −0.184 | 0.183 | 0.183 |
| $d_{31}^\mu \left(\dfrac{pm}{V}\right)$ | −13.015 | 8.559 | 1.152 | −0.826 | −0.773 | 0.558 | 9.042 | 0.097 | −5.853 | −0.130 |
| $G_{33}^\mu$ | 0.360 | −0.041 | −0.303 | 0.103 | 0.360 | −0.041 | −0.303 | −0.303 | 0.103 | 0.103 |
| $d_{33}^\mu \left(\dfrac{pm}{V}\right)$ | −26.682 | 2.322 | 1.892 | −0.466 | −1.584 | 0.151 | 14.858 | 0.160 | −3.304 | −0.074 |

into the crystallographic frame of lithium niobate. The correspondence between this factor 4 and the slope ratio discussed above suggests that the reduction in the acentricity of lithium niobate, introduced by dopants, is mainly due to the number of Li vacancies, fairly independent of the specific impurity used. A similar factor of 4 is also found when regarding the so-called ''threshold'' values[35] for different dopants in lithium niobate which were found to be about 6% in the case of Mg and Zn and about 1.5% in the case of In.[36] The fact that the number of Li vacancies strongly affects the nonlinear optical properties of lithium niobate assures our previous result that the Li places in the crystallographic frame of lithium niobate are the sensitive lattice sites, on which dopants (or vacancies) can modify the dielectric properties most effectively.[20,21] However, this seems to be mainly true for the nonlinear properties (i.e., the acentricity) as the linear dielectric properties behave in a slightly different way: $n_o$ decreases with Mg doping,[37] increases with Zn doping,[38] and decreases with In doping.[16]

Experimental values for the doping dependence of the second order nonlinear susceptibility are to our knowledge only available for Mg-doped congruently grown lithium niobate.[34] The authors show that the tensor coefficients measured ($d_{31}$ and $d_{33}$) are slightly increasing with increasing doping level (0–5 mol %). At first sight this seems to be contradictory to our calculations where a decrease with increasing doping level was found, yet these experimental data strongly support our model in which primarily the number of Li vacancies affects the second order nonlinear susceptibility in lithium niobate. This number of Li vacancies is *increasing* with increasing doping level in *stoichiometric* lithium niobate for which our calculations are made. But, due to the defect structure model of MgO-doped lithium niobate found by Iyi *et al.*,[39] this number of Li vacancies is *decreasing* with increasing Mg doping in *congruently* grown lithium niobate up to a doping level of about 5%. Thus the experimental as well as our calculated data both show that the second order nonlinear susceptibility decreases with increasing number of Li vacancies.

## IV. CONCLUSION

Second order nonlinear optical properties of In-doped lithium niobate single crystals at 1079 nm have been quantitatively studied from the chemical bond viewpoint of crystal materials. The current work shows that introducing $In^{3+}$ cations on Li sites into the crystallographic frame of lithium niobate strongly decreases the second order nonlinear optical response of lithium niobate. This decrease is considerably stronger than for the two-valent dopants Mg and Zn. Yet for all dopants studied so far the effect can be directly referred to the number of Li vacancies accompanying the respective dopants. Thus mainly Li vacancies seem to be responsible for a reduction of the acentricity of the crystal which is connected with the nonlinear optical response. We can further deduce, that Li sites are the sensitive crystal lattices sites that affect dielectric properties of lithium niobate crystals sensitively. Various dopants that are introduced into Li sites successfully modify dielectric properties of lithium niobate crys-

tals. While variations in the nonlinear optical properties seem to be connected with the Li vacancies introduced, changes in the linear properties must be ascribed to the specific ionic characteristics of dopants like In, Mg, and Zn, respectively.

[1] A. Räuber, *Current Topics in Materials Sciences,* edited by E. Kaldis (North Holland, Amsterdam, 1978).

[2] E. Krätzig and O. F. Schirmer, *Photorefractive Materials and Their Applications,* edited by P. Günter and J. P. Huignard (Springer, Berlin, 1988).

[3] G. Zhong, J. Jin, and Z. Wu, Proceedings of the Eleventh International Quantum Electronics, IEEE Cat. No. 80CH1561-0 (1980), p. 631.

[4] T. R. Volk, V. J. Pryalkin, and N. M. Rubinina, Opt. Lett. **15**, 996 (1990).

[5] T. R. Volk and N. M. Rubinina, Ferroelectr. Lett. **14**, 37 (1992).

[6] F. Jermann, M. Simon, and E. Krätzig, J. Opt. Soc. Am. B **12**, 2066 (1995).

[7] A. Lorenzo, H. Jaffrezic, B. Roux, G. Boulon, and J. Garcia-Sole, Appl. Phys. Lett. **67**, 3735 (1995).

[8] T. Volk, M. Wöhlecke, N. Rubinina, A. Reichert, and N. Razumovski, Ferroelectrics **183**, 291 (1996).

[9] G. Malovichko, V. Grachev, E. Kokanyan, and O. Schirmer, Phys. Rev. B **59**, 9113 (1999).

[10] G. Malovichko, V. Grachev, and O. Schirmer, Appl. Phys. B: Lasers Opt. **68**, 785 (1999).

[11] F. P. Safaryan, R. S. Feigelson, and A. M. Petrosyan, J. Appl. Phys. **85**, 8079 (1999).

[12] H. Donnerberg, S. M. Tomlinson, C. R. A. Catlow, and O. F. Schirmer, Phys. Rev. B **44**, 4877 (1991).

[13] Y. Ohkubo, Y. Murakami, T. Saito, A. Yokoyama, S. Uehara, S. Shibata, and Y. Kawase, Phys. Rev. B **60**, 11963 (1999).

[14] D. Xue, K. Betzler, H. Hesse, and D. Lammers, Phys. Status Solidi B **216**, R7 (1999).

[15] T. Volk, M. Wöhlecke, N. Rubinina, N. V. Razumovski, F. Jermann, C. Fischer, and R. Böwer, Appl. Phys. A: Mater. Sci. Process. **60**, 217 (1995).

[16] K. Kasemir, K. Betzler, B. Matzas, B. Tiegel, M. Wöhlecke, N. Rubinina, and T. Volk, Phys. Status Solidi A **166**, R7 (1998).

[17] K. Kasemir, K. Betzler, B. Matzas, B. Tiegel, T. Wahlbrink, M. Wöhlecke, B. Gather, N. Rubinina, and T. Volk, J. Appl. Phys. **84**, 5191 (1998).

[18] D. Xue, K. Betzler, and H. Hesse, J. Phys.: Condens. Matter **12**, 6245 (2000).

[19] D. Xue, K. Betzler, and H. Hesse, Opt. Commun. **182**, 167 (2000).

[20] D. Xue and S. Zhang, Physica B **262**, 78 (1999).

[21] D. Xue and S. Zhang, J. Phys.: Condens. Matter **9**, 7515 (1997).

[22] S. C. Abrahams and P. Marsh, Acta Crystallogr., Sect. B: Struct. Sci. **42**, 61 (1986).

[23] I. D. Brown, Acta Crystallogr., Sect. B: Struct. Sci. **48**, 553 (1992).

[24] J. C. Phillips, Rev. Mod. Phys. **42**, 317 (1970).

[25] J. A. van Vechten, Phys. Rev. **182**, 891 (1969).

[26] B. F. Levine, Phys. Rev. B **7**, 2591 (1973).

[27] H. Neumann, Cryst. Res. Technol. **24**, 815 (1989).

[28] J. M. Merino, R. Diaz, and M. Leon, Phys. Rev. B **61**, 10211 (2000).

[29] B. F. Levine, J. Chem. Phys. **59**, 1463 (1973).

[30] B. F. Levine, Phys. Rev. B **7**, 2600 (1973).

[31] R. Hsu, E. N. Maslen, D. du Boulay, and N. Ishizawa, Acta Crystallogr., Sect. B: Struct. Sci. **53**, 420 (1997).

[32] D. A. Roberts, IEEE J. Quantum Electron. **QE-28**, 2057 (1992).

[33] R. C. Miller, W. A. Norland, and P. M. Bridenbaugh, J. Appl. Phys. **42**, 4145 (1971).

[34] I. Shoji, T. Kondo, A. Kitamoto, M. Shirane, and R. Ito, J. Opt. Soc. Am. B **14**, 2268 (1997).

[35] K. L. Sweeney, L. E. Halliburton, D. A. Bryan, R. Rice, R. Gerson, and H. E. Tomaschke, J. Appl. Phys. **57**, 1036 (1985).

[36] T. R. Volk and M. Wöhlecke, Ferroelectr. Rev. **1**, 195 (1998).

[37] U. Schlarb and K. Betzler, Phys. Rev. **50**, 751 (1994).

[38] U. Schlarb, M. Wöhlecke, B. Gather, A. Reichert, K. Betzler, T. Volk, and N. Rubinina, Opt. Mater. **4**, 791 (1995).

[39] N. Iyi, K. Kitamura, Y. Yajima, S. Kimura, Y. Furukawa, and M. Sato, J. Solid State Chem. **118**, 148 (1995).